Available online at www.sciencedirect.com

ScienceDirect

Biochimica et Biophysica Acta 1768 (2007) 655–668

Biochimica et Biophysica Acta BBA

www.elsevier.com/locate/bbamem

Cholesterol depletion induces dynamic confinement of the G-protein coupled serotonin$_{1A}$ receptor in the plasma membrane of living cells

Thomas J. Pucadyil [1], Amitabha Chattopadhyay *

Centre for Cellular and Molecular Biology, Uppal Road, Hyderabad 500 007, India

Received 1 September 2006; received in revised form 3 January 2007; accepted 4 January 2007
Available online 12 January 2007

Abstract

Cholesterol is an essential constituent of eukaryotic membranes and plays a crucial role in membrane organization, dynamics, function, and sorting. It is often found distributed non-randomly in domains or pools in biological and model membranes and is thought to contribute to a segregated distribution of membrane constituents. Signal transduction events mediated by seven transmembrane domain G-protein coupled receptors (GPCRs) are the primary means by which cells communicate with and respond to their external environment. We analyzed the role of cholesterol in the plasma membrane organization of the G-protein coupled serotonin$_{1A}$ receptor by fluorescence recovery after photobleaching (FRAP) measurements with varying bleach spot sizes. Our results show that lateral diffusion parameters of serotonin$_{1A}$ receptors in normal cells are consistent with models describing diffusion of molecules in a homogenous membrane. Interestingly, these characteristics are altered in cholesterol-depleted cells in a manner that is consistent with dynamic confinement of serotonin$_{1A}$ receptors in the plasma membrane. Importantly, analysis of ligand binding and downstream signaling of the serotonin$_{1A}$ receptor suggests that receptor function is affected in a significantly different manner when intact cells or isolated membranes are depleted of cholesterol. These results assume significance in the context of interpreting effects of cholesterol depletion on diffusion characteristics of membrane proteins in particular, and cholesterol-dependent cellular processes in general.

Keywords: G-protein coupled receptor; Serotonin$_{1A}$ receptor; Cholesterol; Membrane organization and dynamics; FRAP; Beam radius

1. Introduction

Cholesterol is an essential constituent of eukaryotic membranes and plays a crucial role in membrane organization, dynamics, function, and sorting [1,2]. It is often found distributed non-randomly in domains or pools in biological and model membranes and is thought to contribute to a segregated distribution of membrane constituents [1–3]. Cholesterol is proposed to maintain a laterally heterogeneous distribution of lipids and proteins on the plasma membrane due to its putative role in the formation and maintenance of domains such as lipid rafts [4]. Removal of cholesterol from cell membranes is reported to disrupt the integrity of these domains [5], and therefore represents a widely used strategy to disrupt putative functions mediated by these domains. This forms the basis of a number of reports implicating such domains in important cellular functions such as signal transduction [6], and entry of pathogens [7].

Seven transmembrane domain G-protein coupled receptors (GPCRs) constitute one of the largest family of proteins in mammals and account for ~2% of the total proteins coded by the human genome [8]. Signal transduction events mediated by GPCRs are the primary means by which cells communicate with and respond to their external environment [9]. As a consequence, GPCRs represent major targets for the development of novel drug candidates in all clinical areas [10]. The major paradigm in GPCR signaling is that their stimulation leads to the recruitment and activation of heterotrimeric GTP-

Abbreviations: 8-OH-DPAT, 8-hydroxy-2(di-N-propylamino)tetralin; EYFP, enhanced yellow fluorescent protein; FRAP, fluorescence recovery after photobleaching; GPCR, G-protein coupled receptor; IBMX, 3-isobutyl-1-methylxanthine; MβCD, methyl-β-cyclodextrin

* Corresponding author. Tel.: +91 40 2719 2578; fax: +91 40 2716 0311.
E-mail address: amit@ccmb.res.in (A. Chattopadhyay).
[1] Present address: Department of Cell Biology, The Scripps Research Institute, La Jolla, CA 92037, USA.

0005-2736/$ - see front matter © 2007 Elsevier B.V. All rights reserved.
doi:10.1016/j.bbamem.2007.01.002

binding proteins (G-proteins) [11]. These initial events, which are fundamental to all types of GPCR signaling, occur at the plasma membrane via protein–protein interactions. An important consequence is that the organization of molecules such as receptors and G-proteins in the membrane represents an important determinant in GPCR signaling [12,13]. In this regard, the observation that GPCRs are not uniformly present on the plasma membrane but are concentrated in specific membrane domains that are enriched in cholesterol assumes significance [12]. The segregated distribution of GPCRs has given rise to new challenges and complexities in receptor signaling since signaling now has to be understood in context of the two dimensional organization of various signaling components, which include receptors and G-proteins, in the plane of the membrane. The G-protein coupled serotonin$_{1A}$ receptor is the most extensively studied among the serotonin receptors due to the early availability of a selective ligand 8-OH-DPAT that allows extensive biochemical, physiological, and pharmacological characterization of the receptor [14,15]. The functional significance of the serotonin$_{1A}$ receptor is evident from the phenotype exhibited by the mutant (knockout) mice lacking the receptor [16–18]. These mice exhibit enhanced anxiety-related behavior and represent important animal models for the analysis of complex traits such as anxiety disorders and aggression in higher organisms [19].

In this paper, we monitored the membrane organization of the serotonin$_{1A}$ receptor by analyzing its lateral diffusion parameters in the plasma membrane of living cells using the fluorescence recovery after photobleaching (FRAP) approach. In light of the significance of cholesterol in the organization and function of membrane proteins in general, and GPCRs in particular [12,13], we monitored the effect of specific depletion of cholesterol on the lateral diffusion parameters of the serotonin$_{1A}$ receptor. Furthermore, we analyzed ligand binding and downstream signaling of the serotonin$_{1A}$ receptor in normal and cholesterol-depleted cells in order to comprehensively understand the functional significance of the membrane organization of serotonin$_{1A}$ receptors.

2. Materials and methods

2.1. Materials

MβCD, 8-OH-DPAT, penicillin, streptomycin and gentamycin sulfate were obtained from Sigma (St. Louis, MO). D-MEM/F-12 (Dulbecco's Modified Eagle Medium: nutrient mixture F-12 (Ham) (1:1)), fetal calf serum, and geneticin (G 418) were from Invitrogen Life Technologies (Carlsbad, CA). Forskolin and IBMX were from Calbiochem (San Diego, CA). [^{3}H]8-OH-DPAT (sp. activity = 135.0 Ci/mmol) was from DuPont New England Nuclear (Boston, MA). Amplex Red cholesterol assay kit was from Molecular Probes (Eugene, OR). Cyclic AMP [^{3}H] assay kit was from Amersham Biosciences (Buckinghamshire, UK).

2.2. Methods

2.2.1. Cells and cell culture

Chinese hamster ovary (CHO) cells stably expressing the human serotonin$_{1A}$ receptor and the receptor tagged to EYFP (serotonin$_{1A}$-EYFP receptor) were grown in D-MEM/F-12 (1:1) supplemented with 2.4 g/l of sodium bicarbonate, 10% fetal calf serum, 60 μg/ml penicillin, 50 μg/ml streptomycin, 50 μg/ml gentamycin sulfate and 200–300 μg/ml geneticin in a humidified atmosphere with 5% CO_2 at 37 °C. Importantly, the serotonin$_{1A}$ receptor and its tagged form expressed in these cells have been found to be essentially similar to the native serotonin$_{1A}$ receptor expressed in bovine hippocampus in terms of their pharmacology and cellular signaling characteristics [20,21].

2.2.2. Cholesterol depletion of cells in culture

Cells plated at a density of 5×10^5 in 100 mm petridishes were grown for 3 days followed by incubation in serum-free D-MEM/F-12 (1:1) medium for 3 h. Cholesterol depletion was carried out by treating cells with increasing concentrations of MβCD in serum-free D-MEM/F-12 (1:1) medium for 30 min at 37 °C followed by a wash with serum-free D-MEM/F-12 (1:1) medium.

2.2.3. Cholesterol depletion of isolated cell membranes

Cell membranes were isolated by differential centrifugation as described previously [20]. Cell membranes suspended at 1 mg/ml protein concentration were depleted of cholesterol with varying concentrations of MβCD in 50 mM Tris, pH 7.4 buffer at 24 °C with constant shaking for 30 min [22]. Membranes were then spun down at 40,000 × g for 5 min at 4 °C, washed and suspended in 50 mM Tris, pH 7.4 buffer.

2.2.4. Analysis of cholesterol and phospholipid contents

Cholesterol content in cell membranes was estimated using the Amplex Red cholesterol assay kit [23]. Total phospholipid content in these membranes was determined subsequent to digestion with perchloric acid as described earlier [24].

2.2.5. Radioligand binding assays

Receptor binding assay with the radiolabeled agonist [^{3}H]8-OH-DPAT (final concentration = 0.29 nM) was carried out as described previously [20,21]. Saturation binding data were analyzed to estimate the equilibrium dissociation constant (K_d) and maximum binding sites (B_{max}) using the Graphpad Prism software version 4.00 (San Diego, CA).

2.2.6. Cellular signaling assay

Cells plated at a density of 1×10^4 per well of a 24-well plate were grown for 3 days followed by incubation in serum-free D-MEM/F-12 (1:1) medium for 3 h. Cells were then exposed to serum-free D-MEM/F-12 (1:1) medium containing 10 μM forskolin, 50 μM of the phosphodiesterase inhibitor IBMX, and a range (10^{-12} to 10^{-5} M) of concentrations of 8-OH-DPAT at 37 °C for 30 min. The assay was terminated by hypotonic lysis of cells with 10 mM Tris, 5 mM EDTA, pH 7.4 buffer. Cell lysates were boiled for 3 min, brought to room temperature, and spun at 40,000 × g for 10 min at 4 °C to remove precipitated protein. Amount of cAMP in an aliquot of the supernatant was estimated using the Cyclic AMP [^{3}H] assay kit that is based on the protein-binding method [25].

2.2.7. Confocal microscopy and fluorescence recovery after photobleaching (FRAP)

Confocal imaging was carried out on an inverted Zeiss LSM 510 Meta confocal microscope with a Plan-Apochromat 63×, 1.2 NA water-immersion objective using the 514 nm line of an argon laser. Fluorescence emission was collected using the 535–590 nm bandpass filter with the confocal pinhole set between 1 and 2 airy units. Fluorescence distribution analysis of serotonin$_{1A}$-EYFP receptors in response to cholesterol depletion was carried out by imaging the same field of cells before and after treatment with 10 mM MβCD for 30 min in PBS containing Ca^{2+} and Mg^{2+} in an FCS2 closed temperature controlled Bioptechs chamber (Butler, PA) maintained at 37 °C. Fluorescence intensity profiles across a line identically positioned in images acquired before and after cholesterol depletion were analyzed using the Zeiss LSM 510 software (version 3.2). FRAP measurements were performed on cells maintained at 37 °C in PBS containing Ca^{2+} and Mg^{2+} under conditions described previously [21], with a few modifications. The fluorescent periphery of cells that represents the plasma membrane was selected for bleaching and monitoring recovery of fluorescence. The data on diffusion coefficient (D) and mobile fraction (M_f) were calculated from quantitative FRAP experiments where just the bleached region was scanned to achieve improved temporal resolution. The dimensions of the bleach spot were varied by performing FRAP experiments with circular ROIs of different radii. Importantly, recovery of fluorescence intensity was only

monitored from the relatively intense fluorescent cell periphery even though the entire circular ROI placed across the cell periphery was bleached in FRAP experiments. The bleach time point was calculated as the mid-point of the bleach duration. This resulted in the first post-bleach time point starting from a time $t>0$. Data representing the mean fluorescence intensity in the membrane region (obtained using the Zeiss LSM 510 software, version 3.2) within the bleached spot were corrected for background and analyzed. For a two-dimension diffusion model, FRAP data were fit to determine the characteristic diffusion time (τ_d) [26]:

$$F(t) = [F(\infty) - F(0)][\exp(-2\tau_d/t)(I_0(2\tau_d/t) + I_1(2\tau_d/t))] + F(0) \quad (1)$$

where $F(t)$ is the mean background-corrected and normalized fluorescence intensity at time t in the membrane region within the bleached spot, $F(\infty)$ is the recovered fluorescence at time $t\rightarrow\infty$, and $F(0)$ is the bleached fluorescence intensity at time $t\rightarrow 0$. I_0 and I_1 are modified Bessel functions. The effective two-dimensional diffusion coefficient (D_{2D}) is determined from the equation:

$$D_{2D} = \omega^2/4\tau_d \quad (2)$$

where ω is the radius of the bleached spot. For a one-dimension diffusion model, FRAP data were fit to determine the effective one-dimensional diffusion coefficient (D_{1D}) [27]:

$$F(t) = F(\infty)[1 - (\omega^2(\omega^2 + 4\pi D_{1D}t)^{-1})^{1/2}] \quad (3)$$

where ω is the width of the bleach spot. As described earlier [28], $F(0)$ was subtracted from $F(t)$ before FRAP data was fit to Eq. (3). Mobile fraction (M_f) is calculated according to the equation:

$$M_f = [F(\infty) - F(0)]/[F(p) - F(0)] \quad (4)$$

where $F(p)$ is the mean background-corrected and normalized pre-bleach fluorescence intensity. Non-linear curve fitting of fluorescence recovery data to Eqs. (1) and (3) was carried out using the Graphpad Prism software version 4.00 (San Diego, CA). For representation purposes, post-bleach fluorescence intensities in FRAP recovery plots were normalized according to $[F(t)-F(0)]/[F(p)-F(0)]$.

3. Results

3.1. Organization of membrane constituents monitored using FRAP

Monitoring lateral diffusion of molecules in the membrane represents a powerful approach to understand their membrane organization [29,30]. FRAP is a widely used approach to quantitatively estimate diffusion properties of molecules. This approach provides information on the diffusion behavior of an ensemble of molecules, as the area monitored is large (in the order of micrometers) [30,31]. Since fluorescence recovery kinetics in FRAP measurements contains information on the area being monitored, a comprehensive understanding of the spatial organization of molecules in the plasma membrane can be obtained by systematically varying the area monitored in FRAP experiments [31]. Deviations in diffusion characteristics of molecules obtained from FRAP experiments performed with bleach spots of different sizes have been correlated to the presence of domains on the cell surface with dimensions that fall in the same range as the area monitored in these experiments [32–35]. This interpretation is based on the model described below, and has been previously validated by molecular dynamics simulations and FRAP experiments performed on physically domainized model membrane systems [34]. It must be mentioned here that the domains detected by FRAP performed at variable bleach spot sizes must not be confused with domains such as lipid rafts that are currently believed to exist as lateral heterogeneities in the membrane on a spatiotemporal scale far lower than the resolution of FRAP measurements [30].

The recovery of fluorescence into the bleached spot in FRAP experiments is described by two parameters, an apparent diffusion coefficient (D) and mobile fraction (M_f). The rate of fluorescence recovery provides an estimate of the apparent D of molecules, while the extent to which fluorescence recovers provides an estimate of M_f of molecules. Importantly, M_f is only an estimate of the fraction of molecules mobile at the time scale of the FRAP experiment. In general, for molecules diffusing laterally in a homogenous membrane, the diffusion coefficient (D) is independent of the dimensions of the bleach spot in FRAP measurements. A small bleach spot (Fig. 1A) results in faster fluorescence recovery while a large bleach spot (Fig. 1B) results in slower fluorescence recovery, effectively providing a constant value of D. Moreover, if the bleached area is significantly smaller than the total area of the membrane, the extent of fluorescence recovery is the same in both cases resulting in a constant mobile fraction (M_f).

In contrast, if diffusion were confined to closed domains of dimensions that are of the same scale as that of the bleach spot, and static in the time scale of FRAP experiments, D would no longer be a constant. A small bleach spot (Fig. 1C) would tend to monitor diffusion properties of molecules within domains. Thus, kinetics of fluorescence recovery with a small bleach spot on a domainized membrane would be similar to that seen on a homogenous membrane (assuming that the intrinsic membrane properties are similar in the homogenous or domainized state). However, a large bleach spot (overlapping different domains to varying extents, Fig. 1D) would result in non-uniform bleaching of domains since the bleached area would be partial for a few and complete for others. As a consequence, kinetics of fluorescence recovery in the entire region of observation would not be proportional to the actual size of the bleach spot. While kinetics of fluorescence recovery within domains would be proportional to the area bleached in these domains, the apparent D would show an increase (since D is calculated taking into account the actual bleach spot size). Importantly, a large bleach spot would reduce the M_f since it could bleach an entire domain resulting in total loss of fluorescence in such a domain (Fig. 1D).

3.2. Cellular distribution of serotonin$_{1A}$ receptors in normal and cholesterol-depleted cells

We monitored the lateral diffusion properties of the G-protein coupled serotonin$_{1A}$ receptor in the plasma membrane of living cells using such a FRAP approach to detect any possible domain organization and the role of cholesterol in such organization of the receptor. Cholesterol depletion has earlier been reported to affect cellular sorting [36], distribution [37], endocytosis [38] and trafficking [39] of membrane proteins. As a control, we therefore analyzed if the cellular

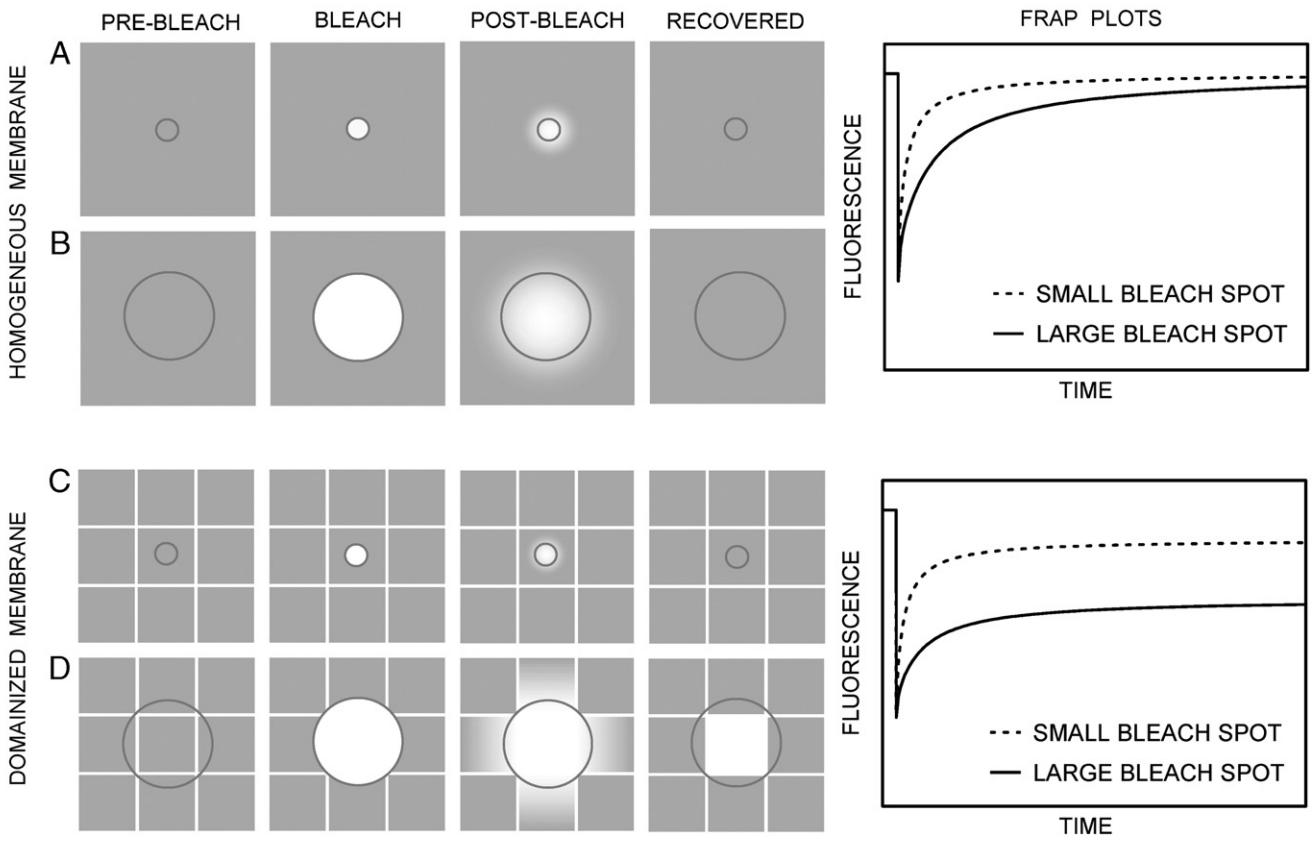

Fig. 1. Possible outcomes of FRAP performed on a homogenous (A and B) and domainized (C and D) membrane with a small (as in panels A and C) or a large (B and D) bleach spot are shown. The circle indicates the region of observation and bleach. Fluorescence recovery kinetics for a small (A) or a large (B) bleach spot on a homogenous membrane is proportional to the size of the spot. Smaller bleach spots result in faster kinetics of fluorescence recovery leading to a constant diffusion coefficient. In addition, if the bleach area is significantly smaller than the total area of the membrane, the extent of fluorescence recovery is the same in both cases resulting in a constant mobile fraction. FRAP measurements on a homogenous membrane therefore show a constant diffusion coefficient and mobile fraction with increasing bleach spot size. In contrast, if diffusion of molecules is confined to closed membrane domains which are static in the time scale of FRAP experiments, the rate of fluorescence recovery for a small (C) or a large (D) bleach spot is no longer proportional to the size of the bleach spot. In this case, florescence recovery kinetics for a small or large bleach spot would be dependent on the area bleached within the domains. This results in an apparent diffusion coefficient that varies with the size of the bleach spot. Larger bleach spots would tend to overestimate the diffusion coefficient since fluorescence recovery kinetics (observed only from diffusion within domains) would be disproportionate to the area bleached. In addition, a large bleach spot (panel D) would reduce the mobile fraction since it would bleach an entire domain resulting in total loss of fluorescence in such a domain. FRAP measurements on such a domainized membrane therefore show an increase in diffusion coefficient and decrease in mobile fraction with increasing bleach spot size. See text for further details.

distribution of serotonin$_{1A}$ receptors was affected due to alterations in cellular cholesterol levels by comparing the fluorescence distribution of serotonin$_{1A}$-EYFP receptors in normal and cholesterol-depleted cells. Cells were depleted of cholesterol using MβCD, a water soluble compound that has previously been shown to selectively extract cholesterol from the plasma membrane by including it in a central non-polar cavity [13]. Confocal mid-plane sections of cells stably expressing serotonin$_{1A}$-EYFP receptors display typical plasma membrane localization characterized by higher fluorescence intensity at the cell periphery (Fig. 2A). The fluorescence distribution in the same group of cells when imaged after cholesterol depletion (using 10 mM MβCD for 30 min at 37 °C), shows no significant differences (Fig. 2B), and is apparent from the similarity in line-profiles of the fluorescence distribution of serotonin$_{1A}$-EYFP receptors in the same group of cells before and after depletion of cholesterol (Fig. 2C and D). Importantly, the mean background-corrected fluorescence intensities at the cell periphery obtained from a large number of unbiased quantitative measurements on normal and cholesterol-depleted cells appear to be similar (Fig. 2E). These results show that cholesterol depletion does not induce any significant alteration in cellular distribution of serotonin$_{1A}$-EYFP receptors in metabolically active cells. Quantitative analysis of the extent of cholesterol depletion upon treatment of cells with increasing concentrations of MβCD is shown in Fig. 2F. Thus, treatment of cells with 10 mM MβCD reduces the cellular cholesterol content by ~41%. The membrane phospholipid content remains unaltered after such treatment thereby indicating the specificity of cholesterol depletion mediated by MβCD under the present conditions. Further, the cholesterol content in cells treated with 10 mM MβCD and maintained in serum-free medium remained ~60% of that in normal cells for a period of 2 h (data not shown). This indicates that within this time frame, analysis of serotonin$_{1A}$ receptor dynamics and function (see later) is not complicated by any significant alteration in the cholesterol content due to cellular biosynthesis. Taken together, these results set up the back-

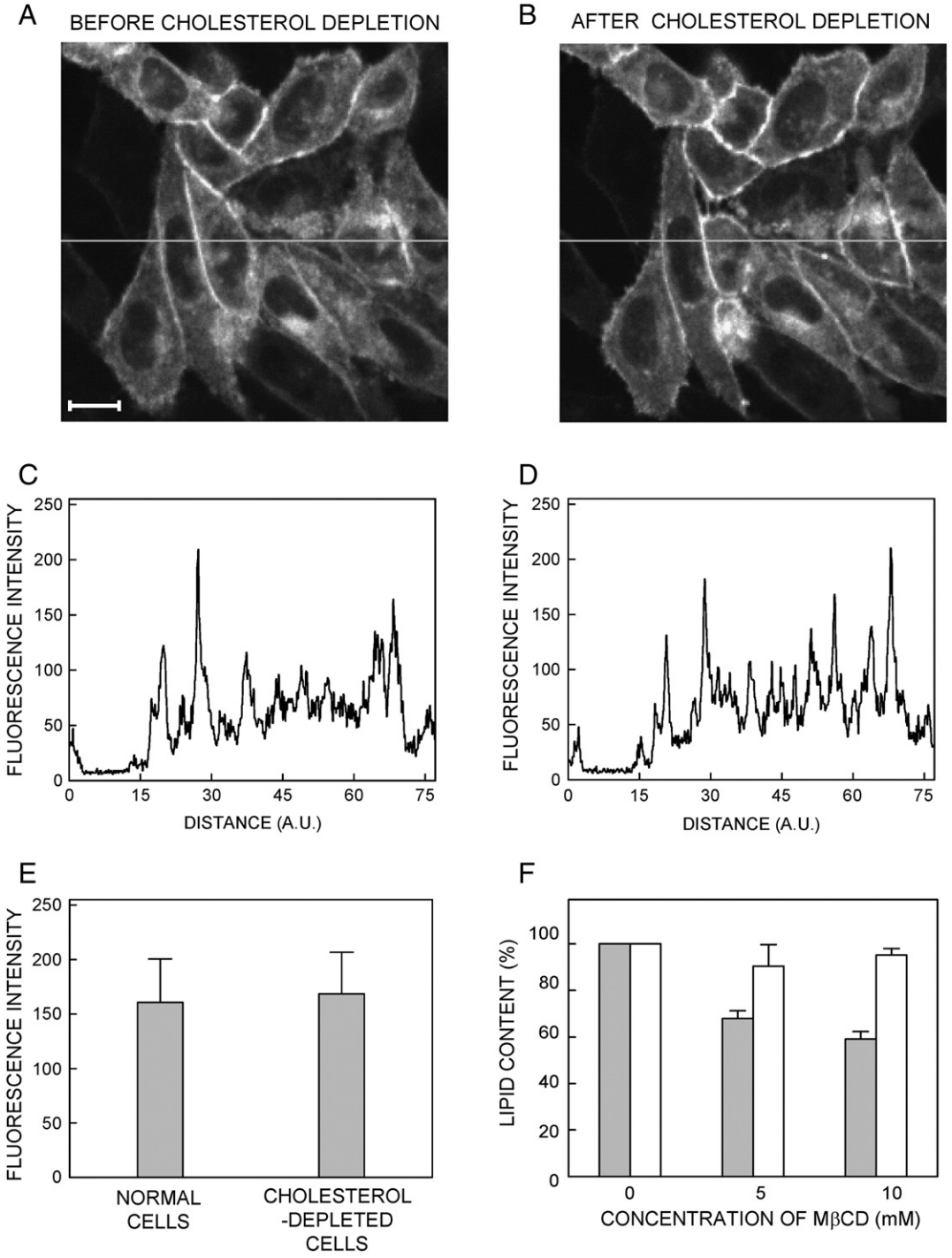

Fig. 2. Confocal micrographs of the same group of cells expressing the serotonin$_{1A}$-EYFP receptor were acquired (A) before and (B) after treatment with 10 mM MβCD for 30 min at 37 °C under identical imaging conditions. The scale bar represents 10 μm. The fluorescence intensity profile across the horizontal line drawn in panels (A) and (B) are shown in panels (C) and (D), respectively. The background-corrected mean fluorescence intensities of serotonin$_{1A}$-EYFP receptors localized in the plasma membrane (fluorescent periphery of cells) in normal and cholesterol-depleted cells are shown in (E). Data represent the means±S.D. of fluorescence intensities measured in 85–87 cells from independent experiments. Quantitative analysis of cholesterol (gray bars) and total phospholipid (white bars) contents assayed in membranes isolated from cells treated with increasing concentrations of MβCD is shown in (F). Data represent the mean±S.E. of at least three independent experiments. See Materials and methods for other details.

ground for FRAP experiments described below on serotonin$_{1A}$-EYFP receptors as they indicate that the analysis of fluorescence recovery is not complicated by any significant alteration in the distribution of receptors in response to cholesterol depletion.

3.3. Membrane organization of serotonin$_{1A}$-EYFP receptors monitored using FRAP

We analyzed the plasma membrane organization of serotonin$_{1A}$-EYFP receptors in living cells maintained at 37 °C

by FRAP measurements with variable bleach spot sizes. Fig. 3A shows a representative experiment performed under imaging conditions optimized to ensure no significant photobleaching of fluorescence during time-lapse imaging. This is apparent from the constant mean fluorescence intensity in region 2 shown in Fig. 3B for the entire duration of the FRAP experiment. It must be mentioned here that while the entire circular ROI was bleached, data on the recovering fluorescence intensity with time was recorded only from the relatively intense fluorescent cell periphery by drawing a mask (shown as the area marked with dotted line in region 1 in Fig. 3A). This ensured that although fluorescence was bleached in an area larger than the plasma membrane, the recovery of fluorescence would predominantly reflect diffusion of serotonin$_{1A}$-EYFP receptors confined to the plasma membrane and not from intracellular regions. The fluorescence recovery kinetics after bleach for spot sizes of radii 1.47 and 3 μm from quantitative FRAP experiments performed on serotonin$_{1A}$-EYFP receptors are shown in Fig. 3C and D.

Analysis of fluorescence recovery kinetics based on a two-dimension diffusion model of serotonin$_{1A}$-EYFP receptors in normal cells with bleach spots of different sizes (radii of 1.47–3 μm) indicates a relatively constant diffusion coefficient (mean±S.D.=0.18±0.02 μm^2 s^{-1}) and mobile fraction M_f (mean±S.D.=73±2%) (Fig. 4A and B). The relatively constant D and M_f over a range of bleach spot sizes in normal cells therefore suggests that serotonin$_{1A}$-EYFP receptors experience a membrane environment that appears homogenous in the spatiotemporal resolution of FRAP measurements (based on conditions described in Fig. 1A and B). It must be mentioned here that we have previously validated FRAP analysis with a range of bleach spot sizes on a homogenous model system of pure GFP in a 90% glycerol–water mixture at 25 °C [40]. The D for such a system was effectively constant across a wide range of bleach spot sizes with an estimated mean of 0.66 μm^2 s^{-1} that is similar to the value of 0.7 μm^2 s^{-1} calculated using the Stokes–Einstein equation in a medium of viscosity corresponding to 90% glycerol–water mixture [41]. Interestingly, FRAP experiments performed on cholesterol-depleted cells with a similar range of bleach spot sizes (1.47–3 μm) show a marked dependence of D and M_f of serotonin$_{1A}$-EYFP receptors on the size of the bleach spot. For example,

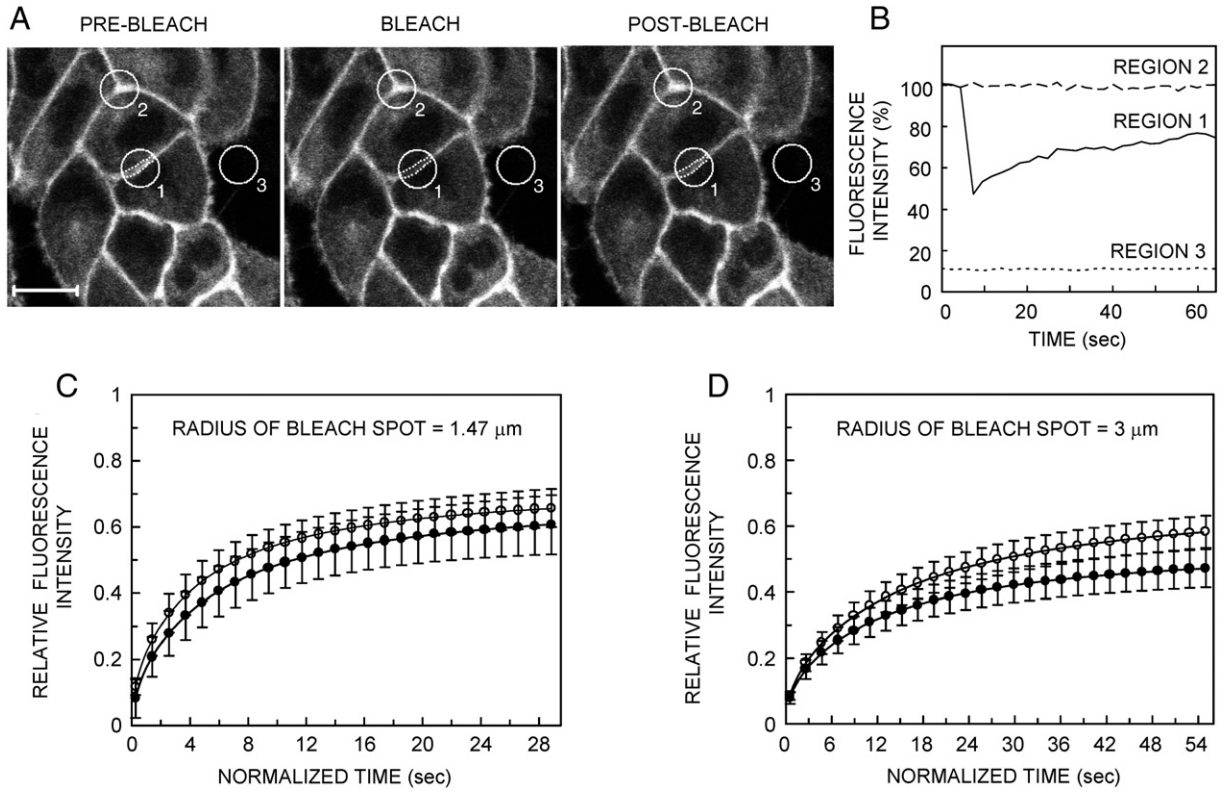

Fig. 3. A representative FRAP experiment performed on cells expressing serotonin$_{1A}$-EYFP receptors. The fluorescent periphery of cells representing the plasma membrane was selected for bleaching and monitoring recovery of fluorescence. Confocal images of the same group of cells before bleach (pre-bleach), immediately after bleach (bleach) and after recovery (post-bleach) for a qualitative FRAP experiment are shown in (A). Region 1 (radius=3 μm) was monitored to measure fluorescence recovery after photobleaching, region 2 to detect any possible bleaching during scanning, and region 3 to monitor background fluorescence. For quantitative FRAP measurements, fluorescence intensity was only monitored from the relatively intense fluorescent cell periphery (shown as the area marked by the dotted line in region 1). The scale bar represents 10 μm. Data representing the normalized mean fluorescence intensities from the regions depicted in (A) for the entire duration of the FRAP experiment are shown in (B). The relatively constant fluorescence intensity in region 2 in (B) shows that the imaging conditions were optimized and no significant photobleaching of fluorescence during time-lapse imaging took place. Fluorescence recovery kinetics of serotonin$_{1A}$-EYFP receptors with bleach spots of (C) 1.47 and (D) 3 μm radius from quantitative FRAP experiments are shown for normal (○) and cholesterol-depleted (●) cells. The data represent means±S.D. of 15–20 independently generated non-linear regression fits of the fluorescence recovery data to Eq. (1) for each bleach spot size. The solid lines are non-linear regression fits of the data to Eq. (1). See Materials and methods for other details.

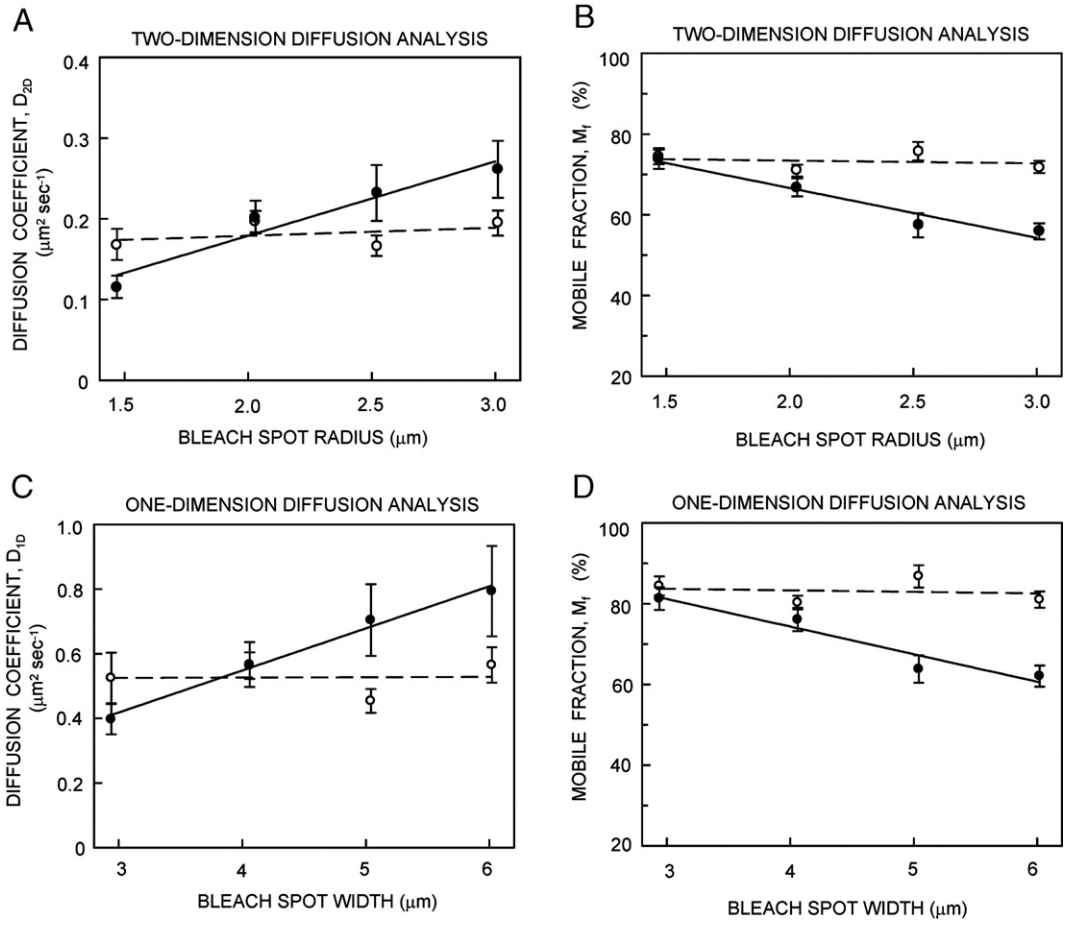

Fig. 4. The diffusion coefficients (A, C) and mobile fractions (B, D) of serotonin$_{1A}$-EYFP receptors obtained from FRAP measurements with bleach spots of different sizes analyzed based on a two-dimension (A, B) or a one-dimension (C, D) diffusion model are shown for normal (–––○–––) and 10 mM MβCD-treated (—●—) cells. Data represent the means±S.E. of 15–20 independent experiments for each bleach spot size. See Materials and methods for other details.

when the area monitored on the plasma membrane is small (bleach spot radius of 1.47 μm), D in cholesterol-depleted cells is ~1.5 fold lower than that in normal cells (Fig. 4A). In contrast, D in cholesterol-depleted cells is ~1.4 fold higher than that in normal cells when the area monitored is large (radius of 3 μm, Fig. 4A). In addition, M_f of serotonin$_{1A}$-EYFP receptors in cholesterol-depleted cells shows a progressive reduction upon increasing the size of the bleach spot. Thus, M_f is reduced by ~22% of its original value in response to a change in bleach spot radius from 1.47 to 3 μm (see Fig. 4B). This type of dependence of D and M_f of the serotonin$_{1A}$-EYFP receptors in cholesterol-depleted membranes is consistent with a model describing confined diffusion in a domainized membrane (see Fig. 1C and D) [32–35]. To the best of our knowledge, this is the first report demonstrating that cholesterol depletion induces dynamic confinement of a transmembrane protein in the plasma membrane of living cells detected using FRAP.

We have earlier monitored the diffusion properties of serotonin$_{1A}$-EYFP receptors by performing FRAP experiments on the surface of attached and well-spread CHO cells [21]. Based on the geometry of bleach on a homogenously fluorescent membrane surface, data from FRAP experiments performed in this manner can be suitably analyzed by a two-dimension diffusion model since fluorescence recovery is expected to be laterally isotropic from all regions around the bleached spot. However, analysis of FRAP experiments performed in this manner on cells stably expressing fluorescently tagged membrane proteins can be complicated due to the unavoidable contribution of fluorescence from intracellular membranes. FRAP experiments performed at the cell periphery would circumvent this problem since fluorescence at the cell periphery would represent serotonin$_{1A}$-EYFP receptors that are predominantly localized in the plasma membrane. The geometry of bleach at the cell periphery would however result in fluorescence recovery being contributed largely due to molecules diffusing across the width of the bleached spot compared to that from above or below the plane of focus. Fluorescence recovery data in such a case may be analyzed based on a model assuming one-dimension diffusion [27,28]. It must be mentioned here that fluorescence recovery kinetics for a one-dimension diffusion process is also proportional to the width of the bleached spot in FRAP experiments. If diffusion of molecules is assumed to occur in a homogenous membrane, a small or a large bleach spot would still provide a constant D. Importantly, analysis of fluorescence recovery kinetics of serotonin$_{1A}$-EYFP receptors in normal and cholesterol-depleted

cells based on a one-dimension diffusion model shows a similar trend as that observed with a two-dimension diffusion model. While FRAP experiments with different bleach spot sizes on serotonin$_{1A}$-EYFP receptors in normal cells provide a relatively constant D (mean ± S.D. = 0.53 ± 0.05 μm^2 s^{-1}) and M_f (mean ± S.D. = 83 ± 3%), similar experiments in cholesterol-depleted cells show that the D and M_f vary significantly with different bleach spot sizes (Fig. 4C and D). Taken together, these results indicate that the dependence of D and M_f on the bleach spot size observed for serotonin$_{1A}$-EYFP receptors in cholesterol-depleted cells is independent of the exact theoretical model (two- or one-dimension diffusion model) used to analyze FRAP data.

The dependence of the lateral diffusion parameters of the serotonin$_{1A}$-EYFP receptors on the bleach spot size in the plasma membrane of cholesterol-depleted cells indicates that cholesterol depletion leads to confined diffusion of serotonin$_{1A}$-EYFP receptors into domains. It would be interesting to comment on the membrane environment (dynamics) in such domains. While FRAP measurements performed with a large bleach spot would suggest the presence or absence of confined diffusion in domains, measurements performed with a small bleach spot would provide information on the lateral diffusion properties of molecules on a local (relatively short) scale either on a homogenous (Fig. 1A) or domainized membrane (Fig. 1C). The diffusion coefficient obtained under such conditions (small bleach spot) could therefore represent an upper limit of the mobility experienced by membrane-bound receptors within domains. We observe that diffusion of serotonin$_{1A}$-EYFP receptors monitored with a small bleach spot in cholesterol-depleted cells is ~1.5 fold lower than that in normal cells (Fig. 4A and C) thereby indicating that serotonin$_{1A}$-EYFP receptors experience a more ordered membrane environment (characterized by lower diffusion) upon depletion of cholesterol. Importantly, since all FRAP experiments were performed on an arbitrary location on the fluorescent periphery of cells, the lower diffusion of serotonin$_{1A}$ receptors obtained from FRAP measurements with a small bleach spot would possibly suggest that the ordered domains cover a significant fraction of the cholesterol-depleted cell surface.

3.4. Serotonin$_{1A}$ receptor function in normal and cholesterol-depleted cells

Cholesterol has been studied quite extensively for its ability to modulate function of membrane receptors [13,42]. As discussed above, FRAP analysis with a small bleach spot indicates that serotonin$_{1A}$ receptors could experience an ordered membrane environment (characterized by lower lateral diffusion) upon cholesterol depletion. In order to analyze the functional consequences of such a change in the membrane environment of serotonin$_{1A}$ receptors in response to cholesterol depletion, we monitored ligand binding of the serotonin$_{1A}$ receptor in membranes isolated from cholesterol-depleted cells. As shown in Fig. 5A, radioligand binding with the specific agonist [^{3}H]8-OH-DPAT suggests that treatment of intact cells with increasing concentrations of MβCD (which leads to increasing extents of cholesterol depletion, see Fig. 2F) leads to an increase in ligand binding of serotonin$_{1A}$ receptors. For example, the specific agonist binding is enhanced by ~51% of the value in normal cells when cells are treated with 10 mM MβCD. As a control, we monitored whether cholesterol depletion of cells expressing the serotonin$_{1A}$-EYFP receptor, used in FRAP experiments, displayed a similar effect. Fig. 5A shows that serotonin$_{1A}$-EYFP receptors also display an increase in the specific agonist binding in response to cholesterol depletion, with a concentration of 10 mM MβCD resulting in a ~83% increase in binding over that found in normal cells. Further, saturation binding analysis (see Table 1) shows that cholesterol depletion with 10 mM MβCD is associated with ~35% decrease in the equilibrium dissociation constant (K_d) and ~16% increase in the maximum number of binding sites (B_{max}) of the agonist to serotonin$_{1A}$ receptors.

Serotonin$_{1A}$ receptor agonists are known to specifically activate the G_i/G_o class of G-proteins in CHO cells thereby inhibiting cAMP synthesis in cells [43]. This is observed in case of normal as well as cholesterol-depleted cells as seen by the progressive decrease in the forskolin-stimulated cAMP levels with increasing concentrations (10^{-12} to 10^{-5} M) of 8-OH-DPAT (Fig. 5B). Parameters obtained from analysis of the concentration-dependent inhibition in forskolin-stimulated cAMP synthesis by the specific agonist 8-OH-DPAT (see Table 2) show that the half maximal inhibition concentration (IC_{50}) value for 8-OH-DPAT in normal cells is ~2.4 nM. Interestingly, despite the enhanced agonist binding of the serotonin$_{1A}$ receptor observed for cholesterol-depleted cells (see Fig. 5A and Table 1), the IC_{50} value for 8-OH-DPAT in cholesterol-depleted cells is ~3 nM, which is similar to that observed in normal cells. These results show that downstream signaling of serotonin$_{1A}$ receptors in response to agonist stimulation remains unaltered upon cholesterol depletion. Interestingly, the stimulatory effect of forskolin on cAMP synthesis appears to be different in normal and cholesterol-depleted cells. Thus, cholesterol-depleted cells generate ~1.3 fold higher levels of cAMP compared to normal cells in response to 10 μM forskolin treatment (see Table 2).

The increase in agonist binding (Fig. 5A) of serotonin$_{1A}$ receptors obtained in membranes isolated from cholesterol-depleted CHO cells appears inconsistent with our earlier results where we reported that cholesterol depletion from native hippocampal membranes endogenously expressing the serotonin$_{1A}$ receptor reduces agonist binding and G-protein coupling of the receptor [22]. A possible reason for such inconsistency could be that the observed increase in agonist binding to serotonin$_{1A}$ receptors could be a result of cholesterol depletion of intact cells in culture and not isolated membranes. To examine this, we monitored the effect of cholesterol depletion of isolated cell membranes on the agonist binding to serotonin$_{1A}$ receptors in such membranes. Fig. 5C shows that treatment of isolated cell membranes with increasing concentrations of MβCD *in vitro* leads to progressive depletion of membrane cholesterol. Interestingly, cholesterol depletion of isolated cell membranes does not lead to an increase in the specific [^{3}H]8-OH-DPAT binding to serotonin$_{1A}$ receptors (Fig. 5D). In fact,

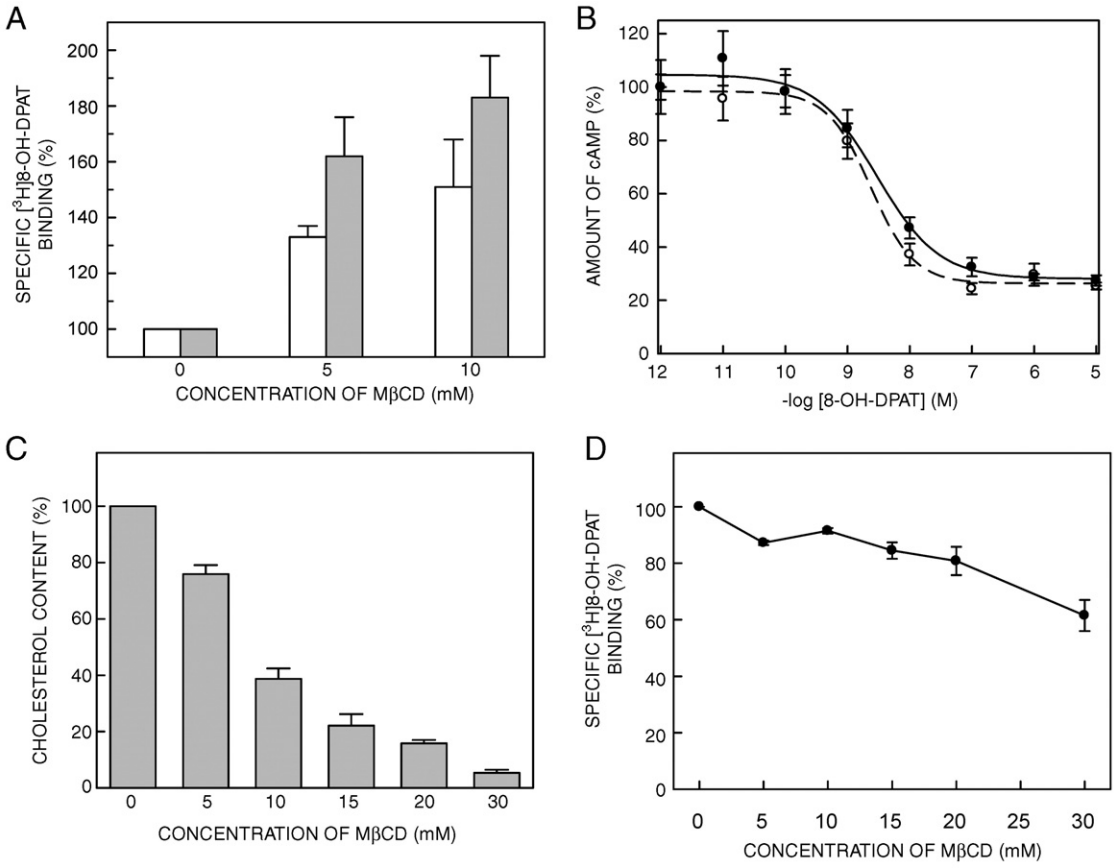

Fig. 5. The specific [^{3}H]8-OH-DPAT binding to serotonin$_{1A}$ (white bars) and serotonin$_{1A}$-EYFP (gray bars) receptors in membranes isolated from cells treated with increasing concentrations of MβCD are shown in (A). Data represent the means±S.E. of at least four independent experiments. Inhibition of the forskolin-stimulated cAMP synthesis mediated by the serotonin$_{1A}$ receptor specific agonist 8-OH-DPAT, monitored in normal (–––○–––) and 10 mM MβCD-treated (—●—) cells, is shown in (B). Values are expressed as percentages of cAMP levels in cells exposed to 10 μM forskolin in the absence of 8-OH-DPAT. Data represent the means±S.E. of at least three independent experiments. The cholesterol contents of isolated cell membranes treated with increasing concentrations of MβCD are shown in (C). Data represent the means±S.E. of three independent experiments. The specific [^{3}H]8-OH-DPAT binding to cell membranes treated with increasing concentrations of MβCD is shown in (D). Data represent the means±S.E. of three independent experiments.

treatment of isolated cell membranes with higher concentrations of MβCD (leading to increasing extents of cholesterol depletion) result in a reduction in the specific agonist binding (Fig. 5D). This result is similar to our previous observations where depletion of cholesterol from isolated native hippocampal membranes led to a reduction in specific agonist binding to serotonin$_{1A}$ receptors [22]. Taken together, these results show that specific agonist binding to serotonin$_{1A}$ receptors is affected in a remarkably different manner depending on whether cells in culture (Fig. 5A) or isolated cell membranes (Fig. 5D) are depleted of cholesterol. Our results show that cholesterol depletion of metabolically active cells does not lead to any significant alteration in the cellular distribution of serotonin$_{1A}$ receptors (see Fig. 2A and B), yet results in an increase in agonist binding to serotonin$_{1A}$ receptors (Fig. 5A). A possible reason for this could be a unique alteration in the membrane environment around the receptor while it is localized in the plasma membrane, which occurs only upon

Table 1
Specific [^{3}H]8-OH-DPAT binding parameters of serotonin$_{1A}$ receptors in cell membranes isolated from normal and cholesterol-depleted cells[a]

Treatment	K_d (nM)	B_{max} (fmol/mg protein)
Normal cells	0.45±0.11	1278±91
Cholesterol-depleted cells[b]	0.30±0.08	1481±51

[a] Binding parameters were calculated by analyzing saturation binding isotherms with a range (0.1–7.5 nM) of radiolabeled [^{3}H]8-OH-DPAT. Data represent means±S.E. of three independent experiments. See Materials and methods for other details.

[b] Cholesterol depletion was performed on cells in culture using 10 mM MβCD. See Materials and methods for other details.

Table 2
Downstream signaling of serotonin$_{1A}$ receptors in normal and cholesterol-depleted cells[a]

Treatment	Forskolin stimulation (% of control)	IC_{50} (nM)
Normal cells	384.3±61.9	2.37±0.39
Cholesterol-depleted cells[b]	500.3±51.4	3.00±0.86

[a] Downstream signaling of the receptor was assayed by monitoring the inhibition in forskolin-stimulated cAMP synthesis in cells in presence of a range (10^{-12} to 10^{-5} M) of concentrations of the specific agonist 8-OH-DPAT. The data represent the means±S.E. of at least three independent experiments. See Materials and methods and Fig. 5B for other details.

[b] Cholesterol depletion was performed on cells in culture using 10 mM MβCD. See Materials and methods for other details.

cholesterol depletion of intact cells in culture and not isolated cell membranes.

4. Discussion

We have recently analyzed the membrane organization of the serotonin$_{1A}$ receptor by monitoring its insolubility in non-ionic detergents utilizing a fluorescence microscopic approach [44,45]. Resistance to solubilization by mild non-ionic detergents such as Triton X-100 at low temperatures represents a widely used biochemical approach to identify, isolate and characterize lipid-rafts, a class of membrane domains enriched in cholesterol and sphingolipids [5]. Significantly, such analysis has indicated that the serotonin$_{1A}$ receptor expressed in CHO cells is predominantly detergent-soluble. While detergent insolubility generally represents the first step in characterizing membrane domains and localization of membrane constituents such as receptors into these domains, concerns associated with such methodologies are the use of low temperatures and the membrane perturbing nature of detergents [46]. In such a scenario, an alternate approach to critically examine the organization of the serotonin$_{1A}$ receptor in an unperturbed cellular environment assumes significance. FRAP measurements performed at variable bleach spot sizes on the serotonin$_{1A}$ receptor in the plasma membrane constitutes one such approach. Results from these measurements in normal cells show nearly constant lateral diffusion parameters with variable bleach spot size thereby indicating that serotonin$_{1A}$ receptors experience a homogenous membrane environment at the spatiotemporal resolution of FRAP measurements. Interestingly, a similar analysis performed on the G-protein coupled neurokinin 2 (NK2) receptor expressed in HEK293 cells has previously shown that it experiences confinement in large scale domains in the plasma membrane [35]. The intrinsic differences in the membrane organization of different members of the GPCR family and/or in different cell types could account for this observation. In addition, dynamic confinement observed in case of the NK2 receptors in cells could be due to the low (20 °C) temperature at which cells were maintained to minimize alterations in the cellular distribution of the receptor in response to stimuli. The low temperature could induce alterations in the membrane structure and/or stabilize interactions between the receptor and cytoskeletal elements underlying the plasma membrane thereby leading to confinement of the receptor in the membrane. This points the need for a comprehensive analysis on multiple GPCRs before attempting to generalize dynamic behavior of GPCRs in living cells. On a broader perspective, these studies emphasize the potential of the FRAP approach performed with variable bleach spot sizes to monitor the organization of membrane constituents in an intact cellular environment.

Cholesterol is proposed to maintain a laterally heterogeneous distribution of lipids and proteins on the plasma membrane due to its putative role in the formation and maintenance of membrane domains [2,3]. Recent observations from a variety of biophysical techniques that monitor membrane dynamics and/or distribution of membrane components on a scale far lower than the resolution of visible light microscopy have indicated the presence of small and dynamic lipid-based heterogeneities in cell membranes which are sensitive to perturbation in the cholesterol and sphingolipid content [47]. Since cholesterol is believed to be the principal constituent of these domains, its removal from cell membranes is reported to disrupt the integrity of these domains [5,6], and therefore represents a widely used strategy to disrupt putative functions mediated by lipid rafts.

Our results indicate that cholesterol depletion induces dynamic confinement of serotonin$_{1A}$ receptors in the plasma membrane based on FRAP experiments with variable bleach spot sizes. Importantly, since the area monitored in FRAP experiments is large (in the order of micrometers), these results suggest a large scale domain organization of the G-protein coupled serotonin$_{1A}$ receptor induced upon depletion of cholesterol from the plasma membrane. The possible mechanisms leading to the reorganization of the plasma membrane resulting in dynamic confinement of the serotonin$_{1A}$ receptor requires further investigation. Interestingly, results from experiments involving cholesterol depletion from model membranes with lipid compositions similar to the plasma membrane, or from the plasma membrane of living cells have previously suggested large scale domain segregation. The role of cholesterol on the segregation of lipid phases has recently been discussed [48]. Thus, in a ternary mixture of saturated phospholipids or sphingolipids with high melting temperatures (T_m), unsaturated phospholipids with low T_m, and cholesterol at 30–50 mol%, increasing extents of cholesterol depletion has been proposed to first lead to the formation of co-existing liquid-ordered (L_o) and liquid-disordered (L_d) phases followed by the co-existence of solid gel-like and L_d phases [48]. Importantly, depletion of cholesterol using β-cyclodextrin from such membranes has been shown to induce segregation of membrane constituents into large domains that can be visualized by fluorescence microscopy [49]. Due to the diversity in lipid composition and the presence of membrane proteins in natural membranes, a challenging question is whether similar phase segregation occurs in response to cholesterol depletion in these membranes. Interestingly, confocal microscopic studies of CHO cells, which have a plasma membrane lipid composition of cholesterol:sphingomyelin:phospholipid of ~40:10:50 (mol%) [50], labeled with membrane phase-specific lipid probes, have indicated a large scale segregation of these probes in the plasma membrane [51]. Furthermore, a comparative analysis of the diffusion behavior of several membrane constituents and the influence of temperature on such behavior in normal and cholesterol-depleted CHO cells have suggested the possibility of formation of solid-ordered membrane phases in cholesterol depleted cells [52]. In addition, cholesterol depletion has been reported to alter the global organization of the cytoskeleton underlying the plasma membrane that is correlated with alterations in the content and distribution of phosphatidylinositol 4,5-bisphosphate (PI(4,5)P2), an organizer of the actin cytoskeleton, in the plasma membrane [53]. It is possible that the removal of cholesterol induces a similar alteration in the distribution of membrane constituents and/or the organization of the cytoske-

leton that effectively leads to dynamic confinement of serotonin$_{1A}$ receptors into domains which were not present on the plasma membrane prior to cholesterol depletion.

The cell surface organization of membrane constituents in relation to their partitioning into cholesterol and sphingolipid enriched domains and/or being confined by the actin cytoskeleton has recently been monitored based on a novel fluorescence correlation spectroscopy (FCS) approach [54]. This study constitutes a systematic analysis of the diffusion time of fluorescent molecules as a function of the observation area in FCS, and is based on the principle of FRAP performed at variable bleach spot sizes [32]. Importantly, such analysis has suggested that transmembrane proteins display characteristics of dynamic confinement in native cell membranes which are relieved upon reducing cellular cholesterol levels and destabilizing the actin cytoskeleton. Although a similar FCS analysis has not been performed with the serotonin$_{1A}$ receptor, a possible reason for the apparent discrepancy between the FCS-based approach and our results could be due to the significantly smaller observation area monitored on the cell membrane with the FCS-based approach (range of observation radii $\omega = \sim 0.2$–0.4 μm [54]) compared to the present FRAP approach (range of bleach spot radii $\omega = 1.47$–3 μm). As mentioned earlier, observations from a variety of biophysical techniques that monitor dynamics and/or distribution of membrane components on a scale far lower than the resolution of visible light microscopy have indicated the presence of small and dynamic lipid-based heterogeneities in cell membranes which are sensitive to perturbation in the cholesterol and sphingolipid content [47]. It is therefore possible that the dynamic confinement of membrane proteins in native membranes and the escape from confinement by cholesterol depletion and actin destabilization observed by FCS could be due to the high spatiotemporal resolution of these measurements. Nevertheless, since FRAP measurements typically monitor diffusion characteristics of molecules on a lower spatiotemporal resolution, any alteration detected in such characteristics can be assumed to reflect a more global (large scale) reorganization of the cell membrane. Based on this rationale, we believe that the consequences of cholesterol depletion could extend beyond its putative effects of disrupting cholesterol- and sphingolipid-rich lipid domains.

It should be noted that FRAP measurements performed with a small bleach spot on a domainized membrane (Fig. 1C) would provide information on the lateral diffusion characteristics of molecules on a relatively local scale (within domains). We observe that diffusion of serotonin$_{1A}$ receptors monitored with a small bleach spot in cholesterol-depleted cells is lower than that in normal cells possibly indicating that serotonin$_{1A}$ receptors experience a more ordered membrane environment (characterized by lower diffusion) upon depletion of cholesterol. Based on our results, we propose a possible model (see Fig. 6) describing dynamic confinement of serotonin$_{1A}$ receptors into ordered domains on the plasma membrane induced upon cholesterol depletion. Importantly, this model is supported by previous analysis based on non-ionic detergent insolubility of serotonin$_{1A}$ receptors which suggested that cholesterol depletion led to a possible reorganization of the receptor into domains that could represent an ordered membrane phase [45]. This proposal was based on the observation that serotonin$_{1A}$ receptors exhibit a higher degree of detergent insolubility in cholesterol-depleted cells [45], and on previous literature where the presence of long chain saturated lipids (that would form an ordered membrane environment) could confer detergent insolubility to membrane constituents in the absence of cholesterol [55–57].

From a lipid–protein interaction perspective, the effect of cholesterol on ligand binding of a variety of G-protein coupled receptors, including the serotonin$_{1A}$ receptor, is well established

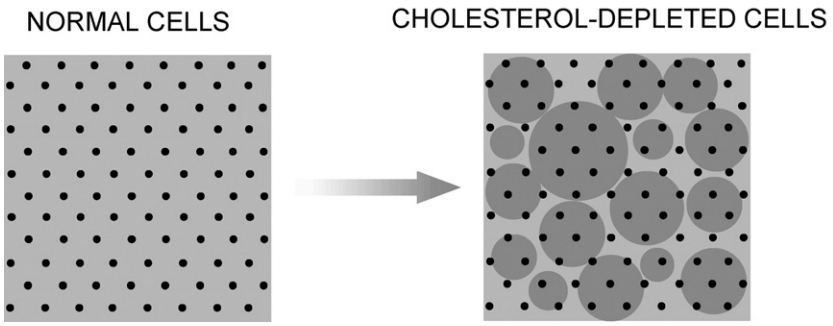

Fig. 6. A model depicting the possible organization of the serotonin$_{1A}$-EYFP receptor in the plasma membrane induced upon cholesterol depletion. The distribution of serotonin$_{1A}$-EYFP receptors (black dots) in the plasma membrane of normal cells is found to be homogenous at the spatiotemporal resolution of FRAP experiments based on the relatively constant diffusion coefficient and mobile fraction of receptors with increasing bleach spot size (Fig. 4). Cholesterol depletion of cells leads to dynamic confinement of receptors into domains (dark gray circles) on the plasma membrane resulting in dependence of diffusion coefficient and mobile fraction of the receptor on the bleach spot size. The distribution of receptors has been depicted to be similar in normal and cholesterol-depleted cells due to the absence of any obvious reorganization of the receptor on the cell surface in response to cholesterol depletion (Fig. 2A and B). FRAP experiments performed on a domainized membrane with a small bleach spot provide information on the diffusion properties of molecules on a relatively local scale (within domains). The lower mobility of serotonin$_{1A}$-EYFP receptors in the plasma membrane of cholesterol-depleted cells determined from FRAP experiments with a small bleach spot indicates that the domains that confine the serotonin$_{1A}$-EYFP receptor (gray circles) represent a relatively ordered environment than other regions of the same membrane. Since FRAP experiments were performed on an arbitrary location on the fluorescent periphery of cells, lower diffusion of the receptors obtained from FRAP measurements with a small bleach spot size would possibly suggest that the ordered domains could cover a significant fraction of the cholesterol-depleted cell surface. Objects depicting receptors and domains are not drawn to scale. See text for further details.

[reviewed in [13]. We observe an increase in ligand binding of the serotonin$_{1A}$ receptor upon depleting cholesterol from cells in culture. Interestingly, similar experiments carried out when isolated cell membranes are depleted of cholesterol do not show such an increase. At the moment, the reasons for such differences on ligand binding to serotonin$_{1A}$ receptors in response to cholesterol depletion can only be speculative. We observe from FRAP experiments, where the area monitored is large (in the order of micrometers), that cholesterol depletion of cells leads to confinement of serotonin$_{1A}$ receptors. Such large scale reorganization appears plausible in membranes that are spatially continuous over such scales and coupled to the cytoskeleton (as in the case of intact cells and not in isolated cell membranes). It is possible that such reorganization due to cholesterol depletion of living cells could alter the immediate membrane environment around the receptor in a manner different from that when isolated cell membranes are depleted of cholesterol. An altered membrane environment around the serotonin$_{1A}$ receptor (possibly more ordered based on results from FRAP experiments with a small bleach spot size, see above) created as a result of cholesterol depletion of intact cells could explain the enhanced agonist binding of the receptor when cells are depleted of cholesterol. It is worthwhile to mention here that previous experiments to solubilize the serotonin$_{1A}$ receptor using detergents such as 3-[(3-cholamidopropyl)-dimethylammonio]-1-propanesulfonate (CHAPS) and 3-[(cholamidopropyl)dimethylammonio]-2-hydroxy-1-propanesulfonate (CHAPSO) have showed that efficient solubilization (as shown by increased ligand binding) of functionally active serotonin$_{1A}$ receptors correlated with the solubilization of lipids with a markedly higher presence of saturated fatty acyl chains [58,59]. Interestingly, such solubilization is accompanied by depletion of membrane cholesterol [60]. Taken together, these results indicate that an ordered membrane environment (characterized by enrichment in lipids with saturated fatty acyl chains) and lacking cholesterol could contribute to enhanced ligand binding of the serotonin$_{1A}$ receptor.

We extended our analysis of the role of cholesterol in the function of serotonin$_{1A}$ receptors by monitoring the effects of cholesterol depletion on its downstream signaling in cells. Interestingly, the function of molecules involved in GPCR signaling such as G-proteins and adenylyl cyclase, have earlier been found to be dependent on the membrane cholesterol content. A reduction in the cholesterol content has previously been shown to reduce the intrinsic GTPase activity of $G_{\alpha i}$ proteins [61]. Moreover, adenylyl cyclase has been found to display enhanced activity in cholesterol-depleted cardiomyocytes [62], a result similar to what we observe [see Fig. 5D). Thus, interpretations on the specific role of cholesterol in signaling functions of serotonin$_{1A}$ receptors could be complicated by the distinct effects of cholesterol depletion on the function of other partners in GPCR signal transduction. Our results show that downstream signaling of serotonin$_{1A}$ receptors upon stimulation with the agonist remains largely unaltered in cholesterol-depleted cells despite the effects of cholesterol depletion on membrane organization and agonist binding to serotonin$_{1A}$ receptors. A possible reason for this could be the induction of multiple cellular responses that independently modulate cAMP levels in cells. Thus, the effect of an increase in agonist binding of serotonin$_{1A}$ receptors due to cholesterol depletion could be effectively diminished by the concomitant increase in cAMP levels by receptor-independent pathway in cells thereby leading to no apparent change in the concentration-dependent inhibition of cAMP levels upon stimulation of the serotonin$_{1A}$ receptor with the agonist in normal and cholesterol-depleted cells.

Our results indicate that a reduction in membrane cholesterol content can induce significant changes in the plasma membrane organization of the serotonin$_{1A}$ receptor. Whether such an alteration in membrane cholesterol content is physiologically relevant represents an important question. Previous literature suggests that chronic administration of cholesterol-lowering drugs like statins results in the specific reduction of neuronal membrane cholesterol levels *in vivo*, leaving serum cholesterol levels unaffected [63]. Importantly, low serum cholesterol concentration has been correlated with an increase in the prevalence of suicide in humans [64], and is partly attributed to an altered serotonin metabolism [65]. Our present results on the effect of a reduction in membrane cholesterol levels on the organization and function of the serotonin$_{1A}$ receptor could therefore provide an explanation behind the etiology of psychological disorders that are correlated with an altered cholesterol metabolism. We are currently exploring the consequences of statin-induced reduction in membrane cholesterol levels on the organization and function of the serotonin$_{1A}$ receptor. Our preliminary results suggest that even modest levels of cholesterol reduction achieved using statins can induce significant alterations in the membrane organization and function of the serotonin$_{1A}$ receptor [T.J. Pucadyil, S. Shrivastava, S. Ganguly, and A. Chattopadhyay, unpublished results].

In summary, our results show that cholesterol has an important role in the global membrane organization and function of the serotonin$_{1A}$ receptor. These results constitute the first report on the membrane organization of the serotonin$_{1A}$ receptor in the plasma membrane of living cells monitored by a non-perturbing fluorescence-based approach. On a broader perspective, our results assume significance in understanding the modulatory role of the membrane lipid environment on the organization and function of other G-protein coupled transmembrane receptors.

Acknowledgements

This work was supported by research grants from the Council of Scientific and Industrial Research, Government of India, to A. C. T. J. P. thanks the Council of Scientific and Industrial Research for the award of a Senior Research Fellowship. We thank Sandra L. Schmid and members of the Chattopadhyay lab for their helpful comments on the manuscript. We gratefully acknowledge Sadashiva S. Karnik for the serotonin$_{1A}$-EYFP receptor construct, and Nandini Rangaraj, V. K. Sarma, N.R. Chakravarthi and K.N. Rao for help with confocal microscopy.

References

[1] F. Schroeder, J.K. Woodford, J. Kavecansky, W.G. Wood, C. Joiner, Cholesterol domains in biological membranes, Mol. Membr. Biol. 12 (1995) 113–119.

[2] O.G. Mouritsen, M.J. Zuckermann, What's so special about cholesterol? Lipids 39 (2004) 1101–1113.

[3] S. Mukherjee, F.R. Maxfield, Membrane domains, Annu. Rev. Cell Dev. Biol. 20 (2004) 839–866.

[4] R.G. Anderson, K. Jacobson, A role for lipid shells in targeting proteins to caveolae, rafts, and other lipid domains, Science 296 (2002) 1821–1825.

[5] D.A. Brown, E. London, Structure and function of sphingolipid and cholesterol-rich membrane rafts, J. Biol. Chem. 275 (2000) 17221–17224.

[6] K. Simons, D. Toomre, Lipid rafts and signal transduction, Nat. Rev., Mol. Cell Biol. 1 (2000) 31–39.

[7] F.G. van der Goot, T. Harder, Raft membrane domains: from a liquid-ordered membrane phase to a site of pathogen attack, Semin. Immunol. 13 (2001) 89–97.

[8] R. Fredriksson, M.C. Lagerström, L.-G. Lundin, H.B. Schiöth, The G-protein-coupled receptors in the human genome form five main families. Phylogenetic analysis, paralogon groups, and fingerprints, Mol. Pharmacol. 63 (2003) 1256–1272.

[9] K.L. Pierce, R.T. Premont, R.J. Lefkowitz, Seven-transmembrane receptors, Nat. Rev., Mol. Cell Biol. 3 (2002) 639–650.

[10] A.L. Hopkins, C.R. Groom, The druggable genome, Nat. Rev., Drug Discov. 1 (2002) 727–730.

[11] H.E. Hamm, How activated receptors couple to G proteins, Proc. Natl. Acad. Sci. U. S. A. 98 (2001) 4819–4821.

[12] R.S. Ostrom, P.A. Insel, The evolving role of lipid rafts and caveolae in G protein-coupled receptor signaling: implications for molecular pharmacology, Br. J. Pharmacol. 143 (2004) 235–245.

[13] T.J. Pucadyil, A. Chattopadhyay, Role of cholesterol in the function and organization of G-protein coupled receptors, Prog. Lipid Res. 45 (2006) 295–333.

[14] J.R. Raymond, Y.V. Mukhin, T.W. Gettys, M.N. Garnovskaya, The recombinant 5-HT1A receptor: G protein coupling and signalling pathways, Br. J. Pharmacol. 127 (1999) 1751–1764.

[15] T.J. Pucadyil, S. Kalipatnapu, A. Chattopadhyay, The serotonin$_{1A}$ receptor: a representative member of the serotonin receptor family, Cell. Mol. Neurobiol. 25 (2005) 553–580.

[16] S. Ramboz, R. Oosting, D.A. Amara, H.-F. Kung, P. Blier, M. Mendelsohn, J.J. Mann, D. Brunner, R. Hen, Serotonin receptor 1A knockout: an animal model of anxiety-related disorder, Proc. Natl. Acad. Sci. U. S. A. 95 (1998) 14476–14481.

[17] L.K. Heisler, H.-M. Chu, T.J. Brennan, J.A. Danao, P. Bajwa, L.H. Parsons, L.H. Tecott, Elevated anxiety and antidepressant-like responses in serotonin 5-HT$_{1A}$ receptor mutant mice, Proc. Natl. Acad. Sci. U. S. A. 95 (1998) 15049–15054.

[18] C.L. Parks, P.S. Robinson, E. Sibille, T. Shenk, M. Tóth, Increased anxiety of mice lacking the serotonin$_{1A}$ receptor, Proc. Natl. Acad. Sci. U. S. A. 95 (1998) 10734–10739.

[19] J.A. Gingrich, R. Hen, Dissecting the role of the serotonin system in neuropsychiatric disorders using knockout mice, Psychopharmacology 155 (2001) 1–10.

[20] S. Kalipatnapu, T.J. Pucadyil, K.G. Harikumar, A. Chattopadhyay, Ligand binding characteristics of the human serotonin$_{1A}$ receptor heterologously expressed in CHO cells, Biosci. Rep. 24 (2004) 101–115.

[21] T.J. Pucadyil, S. Kalipatnapu, K.G. Harikumar, N. Rangaraj, S.S. Karnik, A. Chattopadhyay, G-protein-dependent cell surface dynamics of the human serotonin$_{1A}$ receptor tagged to yellow fluorescent protein, Biochemistry 43 (2004) 15852–15862.

[22] T.J. Pucadyil, A. Chattopadhyay, Cholesterol modulates ligand binding and G-protein coupling to serotonin$_{1A}$ receptors from bovine hippocampus, Biochim. Biophys. Acta 1663 (2004) 188–200.

[23] D.M. Amundson, M. Zhou, Fluorometric method for the enzymatic determination of cholesterol, J. Biochem. Biophys. Methods 38 (1999) 43–52.

[24] C.W.F. McClare, An accurate and convenient organic phosphorus assay, Anal. Biochem. 39 (1971) 527–530.

[25] C. Norstedt, B.B. Fredholm, A modification of a protein-binding method for rapid quantification of cAMP in cell-culture supernatants and body fluid, Anal. Biochem. 189 (1990) 231–234.

[26] D.M. Soumpasis, Theoretical analysis of fluorescence photobleaching recovery experiments, Biophys. J. 41 (1983) 95–97.

[27] J. Ellenberg, E.D. Siggia, J.E. Moreira, C.L. Smith, J.F. Presley, H.J. Worman, J. Lippincott-Schwartz, Nuclear membrane dynamics and reassembly in living cells: targeting of an inner nuclear membrane protein in interphase and mitosis, J. Cell Biol. 138 (1997) 1193–1206.

[28] E.D. Siggia, J. Lippincott-Schwartz, S. Bekiranov, Diffusion in inhomogeneous media: theory and simulations applied to whole cell photobleach recovery, Biophys. J. 79 (2000) 1761–1770.

[29] A. Kusumi, H. Ike, C. Nakada, K. Murase, T. Fujiwara, Single-molecule tracking of membrane molecules: plasma membrane compartmentalization and dynamic assembly of raft-philic signaling molecules, Semin. Immunol. 17 (2005) 3–21.

[30] B.C. Lagerholm, G.E. Weinreb, K. Jacobson, N.L. Thompson, Detecting microdomains in intact cell membranes, Annu. Rev. Phys. Chem. 56 (2005) 309–336.

[31] M. Edidin, Patches, posts and fences: proteins and plasma membrane domains, Trends Cell Biol. 2 (1992) 376–380.

[32] E. Yechiel, M. Edidin, Micrometer-scale domains in fibroblast plasma membranes, J. Cell Biol. 105 (1987) 755–760.

[33] M. Edidin, I. Stroynowski, Differences between the lateral organization of conventional and inositol phospholipid-anchored membrane proteins. A further definition of micrometer scale membrane domains, J. Cell Biol. 112 (1991) 1143–1150.

[34] L. Salomé, J.L. Cazeils, A. Lopez, J.F. Tocanne, Characterization of membrane domains by FRAP experiments at variable observation areas, Eur. Biophys. J. 27 (1998) 391–402.

[35] L. Cézanne, S. Lecat, B. Lagane, C. Millot, J.Y. Vollmer, H. Matthes, J.L. Galzi, A. Lopez, Dynamic confinement of NK2 receptors in the plasma membrane. Improved FRAP analysis and biological relevance, J. Biol. Chem. 279 (2004) 45057–45067.

[36] G.H. Hansen, L. Niels-Christiansen, E. Thorsen, L. Immerdal, E.M. Danielsen, Cholesterol depletion of enterocytes: effect on the golgi complex and apical membrane trafficking, J. Biol. Chem. 275 (2000) 5136–5142.

[37] L.J. Pike, L. Casey, Cholesterol levels modulate EGF receptor-mediated signaling by altering receptor function and trafficking, Biochemistry 41 (2002) 10315–10322.

[38] A. Subtil, I. Gaidarov, K. Kobylarz, M.A. Lampson, J.H. Keen, T.E. McGraw, Acute cholesterol depletion inhibits clathrin-coated pit budding, Proc. Natl. Acad. Sci. U. S. A. 96 (1999) 6775–6780.

[39] M.F. Pediconi, C.E. Gallegos, E.B. De Los Santos, F.J. Barrantes, Metabolic cholesterol depletion hinders cell-surface trafficking of the nicotinic acetylcholine receptor, Neuroscience 128 (2004) 239–249.

[40] T.J. Pucadyil, A. Chattopadhyay, Confocal fluorescence recovery after photobleaching of green fluorescent protein in solution, J. Fluoresc. 16 (2006) 87–94.

[41] U. Kubitscheck, O. Kückman, T. Kues, R. Peters, Imaging and tracking of single GFP molecules in solution, Biophys. J. 78 (2000) 2170–2179.

[42] K. Burger, G. Gimpl, F. Fahrenholz, Regulation of receptor function by cholesterol, Cell. Mol. Life Sci. 57 (2000) 1577–1592.

[43] J.R. Raymond, C.L. Olsen, T.W. Gettys, Cell-specific physical and functional coupling of human 5-HT$_{1A}$ receptors to inhibitory G protein alpha-subunits and lack of coupling to G_s alpha, Biochemistry 32 (1993) 11064–11073.

[44] S. Kalipatnapu, A. Chattopadhyay, A GFP fluorescence-based approach to determine detergent insolubility of the human serotonin$_{1A}$ receptor, FEBS Lett. 576 (2004) 455–460.

[45] S. Kalipatnapu, A. Chattopadhyay, Membrane organization of the human serotonin$_{1A}$ receptor monitored by detergent insolubility using GFP fluorescence, Mol. Membr. Biol. 22 (2005) 539–547.

[46] M. Edidin, The state of lipid rafts: from model membranes to cells, Annu. Rev. Biophys. Biomol. Struct. 32 (2003) 257–283.

[47] S. Mayor, M. Rao, Rafts: scale-dependent, active lipid organization at the cell surface, Traffic 5 (2004) 231–240.

[48] E. London, How principles of domain formation in model membranes may explain ambiguities concerning lipid raft formation in cells, Biochim. Biophys. Acta 1746 (2005) 203–220.
[49] S.L. Veatch, S.L. Keller, Separation of liquid phases in giant vesicles of ternary mixtures of phospholipids and cholesterol, Biophys. J. 85 (2003) 3074–3083.
[50] D.E. Warnock, C. Roberts, M.S. Lutz, W.A. Blackburn, W.W. Young Jr., J.U. Baenziger, Determination of plasma membrane lipid mass and composition in cultured Chinese hamster ovary cells using high gradient magnetic affinity chromatography, J. Biol. Chem. 268 (1993) 10145–10153.
[51] M. Hao, S. Mukherjee, F.R. Maxfield, Cholesterol depletion induces large scale domain segregation in living cell membranes, Proc. Natl. Acad. Sci. U. S. A. 98 (2001) 13072–13077.
[52] S.Y. Nishimura, M. Vrljic, L.O. Klein, H.M. McConnell, W.E. Moerner, Cholesterol depletion induces solid-like regions in the plasma membrane, Biophys. J. 90 (2006) 927–938.
[53] J. Kwik, S. Boyle, D. Fooksman, L. Margolis, M.P. Sheetz, M. Edidin, Membrane cholesterol, lateral mobility, and the phosphatidylinositol 4,5-bisphosphate-dependent organization of cell actin, Proc. Natl. Acad. Sci. U. S. A. 100 (2003) 13964–13969.
[54] P.-F. Lenne, L. Wawrezinieck, F. Conchonaud, O. Wurtz, A. Boned, X.J. Guo, H. Rigneault, H.T. He, D. Marguet, Dynamic molecular confinement in the plasma membrane by microdomains and the cytoskeleton meshwork, EMBO J. 25 (2006) 3245–3256.
[55] R.J. Schroeder, S.N. Ahmed, Y. Zhu, E. London, D.A. Brown, Cholesterol and sphingolipid enhance the Triton X-100 insolubility of glycosyl-phosphatidylinositol-anchored proteins by promoting the formation of detergent-insoluble ordered membrane domains, J. Biol. Chem. 273 (1998) 1150–1157.
[56] T.J. Pucadyil, A. Chattopadhyay, Exploring detergent insolubility in bovine hippocampal membranes: a critical assessment of the requirement for cholesterol, Biochim. Biophys. Acta 1661 (2004) 9–17.
[57] S. Keller, A. Tsamaloukas, H. Heerklotz, A quantitative model describing the selective solubilization of membrane domains, J. Am. Chem. Soc. 127 (2005) 11469–11476.
[58] P. Banerjee, J.T. Buse, G. Dawson, Asymmetric extraction of membrane lipids by CHAPS, Biochim. Biophys. Acta 1044 (1990) 305–314.
[59] P. Banerjee, G. Dawson, A. Dasgupta, Enrichment of saturated fatty acid containing phospholipids in sheep brain serotonin receptor preparations: use of microwave irradiation for rapid transesterification of phospholipids, Biochim. Biophys. Acta 1110 (1992) 65–74.
[60] A. Chattopadhyay, Md. Jafurulla, S. Kalipatnapu, T.J. Pucadyil, K.G. Harikumar, Role of cholesterol in ligand binding and G-protein coupling of serotonin1A receptors solubilized from bovine hippocampus, Biochem. Biophys. Res. Commun. 327 (2005) 1036–1041.
[61] S. Ropero, A. Chiloeches, A. Montes, M.J. Toro-Nozal, Cholesterol cell content modulates GTPase activity of G proteins in GH4C1 cell membranes, Cell. Signal. 15 (2003) 131–138.
[62] V.O. Rybin, X. Xu, M.P. Lisanti, S.F. Steinberg, Differential targeting of the β-adrenergic receptor subtypes and adenylyl cyclase to cardiomyocyte caveolae, J. Biol. Chem. 275 (2000) 41447–41457.
[63] C. Kirsch, G.P. Eckert, W.E. Mueller, Statin effects on cholesterol micro-domains in brain plasma membranes, Biochem. Pharmacol. 65 (2003) 843–856.
[64] P.H.A. Steegmans, D. Fekkes, A.W. Hoes, A.A.A. Bak, E. van der Does, D.E. Grobbee, Low serum cholesterol concentration and serotonin metabolism in men, Br. Med. J. 312 (1996) 221.
[65] M. Zureik, D. Courbon, P. Ducimetière, Serum cholesterol concentration and death from suicide in men: Paris prospective study I, Br. Med. J. 313 (1996) 649–651.